

THE STELLAR CONTENT OF RICH YOUNG CLUSTERS IN THE LARGE MAGELLANIC CLOUD

REBECCA A. W. ELSON,¹ S. MICHAEL FALL,^{2,3} AND KENNETH C. FREEMAN^{2,4}

Received 1987 December 15; accepted 1988 July 6

ABSTRACT

We present luminosity functions for six rich star clusters in the Large Magellanic Cloud (LMC) with ages $3\text{--}5 \times 10^7$ yr. The luminosity functions are derived from star counts on photographic plates with various limiting magnitudes, and extend over the mass range $1.5 \lesssim m/M_{\odot} \lesssim 6$. The corresponding initial mass functions (IMFs) are considerably flatter than the Salpeter IMF, and there is some evidence for small variations in the slope of the mass function from cluster to cluster. We also present luminosity functions for the field stars surrounding each cluster; as expected, these are steeper than the luminosity functions of the clusters since the fields include stars with a greater range of ages. We compare the IMFs of the LMC clusters with those of Galactic open and globular clusters and discuss some of the implications of our results. In a recent study, Mateo (1988) finds steep mass functions for a different sample of rich clusters in the Magellanic Clouds. Unfortunately only a limited comparison can be made between our results and his, but there are no obvious conflicts. Further observations are needed to determine whether the IMFs have large variations from one cluster to another. If the IMFs are generally as flat as those found here, then the mass-to-light ratios of the clusters may be smaller than was previously thought; this strengthens our suggestion in an earlier paper that the young LMC clusters overflow their tidal limits. Flat IMFs also imply that stellar winds, supernovae, and other stellar ejecta play important roles in the early evolution of the clusters and may be responsible for the unbound halos.

Subject headings: clusters: open — galaxies: Magellanic Clouds — galaxies: stellar content — luminosity function

I. INTRODUCTION

Observations of stellar initial mass functions (IMFs) in different environments are crucial for guiding theories that seek to explain star formation. Since many field stars were born in clusters or associations, understanding star formation on this scale is necessary to explain global IMFs in galaxies. Furthermore, clusters are particularly simple to study, since the stars are approximately coeval. The IMF is also of prime importance for understanding the formation and early evolution of star clusters. It governs the input of energy into a protocluster by stellar winds and supernovae, the production of heavy elements and possible self-enrichment, and the rate of mass loss through stellar evolution. IMFs have been estimated for both open and globular clusters in the Milky Way (see McClure *et al.* 1986; Scalo 1986). There is no strong evidence for variations in the IMFs of open clusters, but the uncertainties are large as the result of small numbers of stars. In globular clusters, the IMFs appear to vary considerably from one cluster to another and may be correlated with metallicity.

The rich young clusters in the Large Magellanic Cloud (LMC) provide an ideal opportunity to extend the study of IMFs to other galaxies. They are only slightly less massive than the globular clusters in the Milky Way, but in several other respects they resemble the Galactic open clusters (Freeman, Illingworth, and Oemler 1983; Elson and Fall 1985*a, b*; Elson, Fall, and Freeman 1987, hereafter Paper I). Flower *et al.* (1980) and Nelson and Hodge (1983) present

luminosity functions for two LMC clusters, NGC 1868 (7×10^8 yr) and NGC 1847 (2.5×10^7 yr), but do not convert them to mass functions. Melnick (1985) has studied the IMF of NGC 2070, the rich cluster in the 30 Dor nebula. Freeman (1977) discusses the IMFs of six young LMC clusters; his results are superseded by those presented here. After completing most of the work described in this paper, we learned of a recent study by Mateo (1988) of the IMFs of six rich clusters in the Magellanic Clouds.

We have determined the IMFs of the following LMC clusters: NGC 1866, NGC 2214, NGC 2156, NGC 2159, NGC 2164, and NGC 2172. Their positions on the sky are shown in Figure 1. The last four are located close together and are referred to here as the "Quartet." The clusters in our sample are among the richest in the LMC. They have masses $\sim 10^4\text{--}10^5 M_{\odot}$, central densities $\sim 10^2 M_{\odot} \text{pc}^{-3}$, and extend to radii ~ 80 pc (Paper I). Their ages are $3\text{--}5 \times 10^7$ yr, and any age spreads within the clusters are estimated to be small in comparison (Robertson 1974*a*). The clusters are dynamically well mixed, but are not relaxed through two-body encounters (Paper I). Little or no mass segregation is observed at the relevant range of radii, and, together with the small age spreads, this makes the interpretation of the IMFs relatively straightforward.

In § II we describe our data and derive luminosity functions for the LMC clusters and surrounding fields. In § III we use stellar evolution models to convert the cluster luminosity functions to mass functions. Section IV contains a comparison between our results and those for other clusters in the Magellanic Clouds and in the Milky Way. In § V we estimate mass-to-light ratios of the clusters from stellar population models and calculate their total masses, central densities, and evolutionary

¹ The Institute for Advanced Study.

² Space Telescope Science Institute.

³ Department of Physics and Astronomy, The Johns Hopkins University.

⁴ Mount Stromlo and Siding Spring Observatory, The Australian National University.

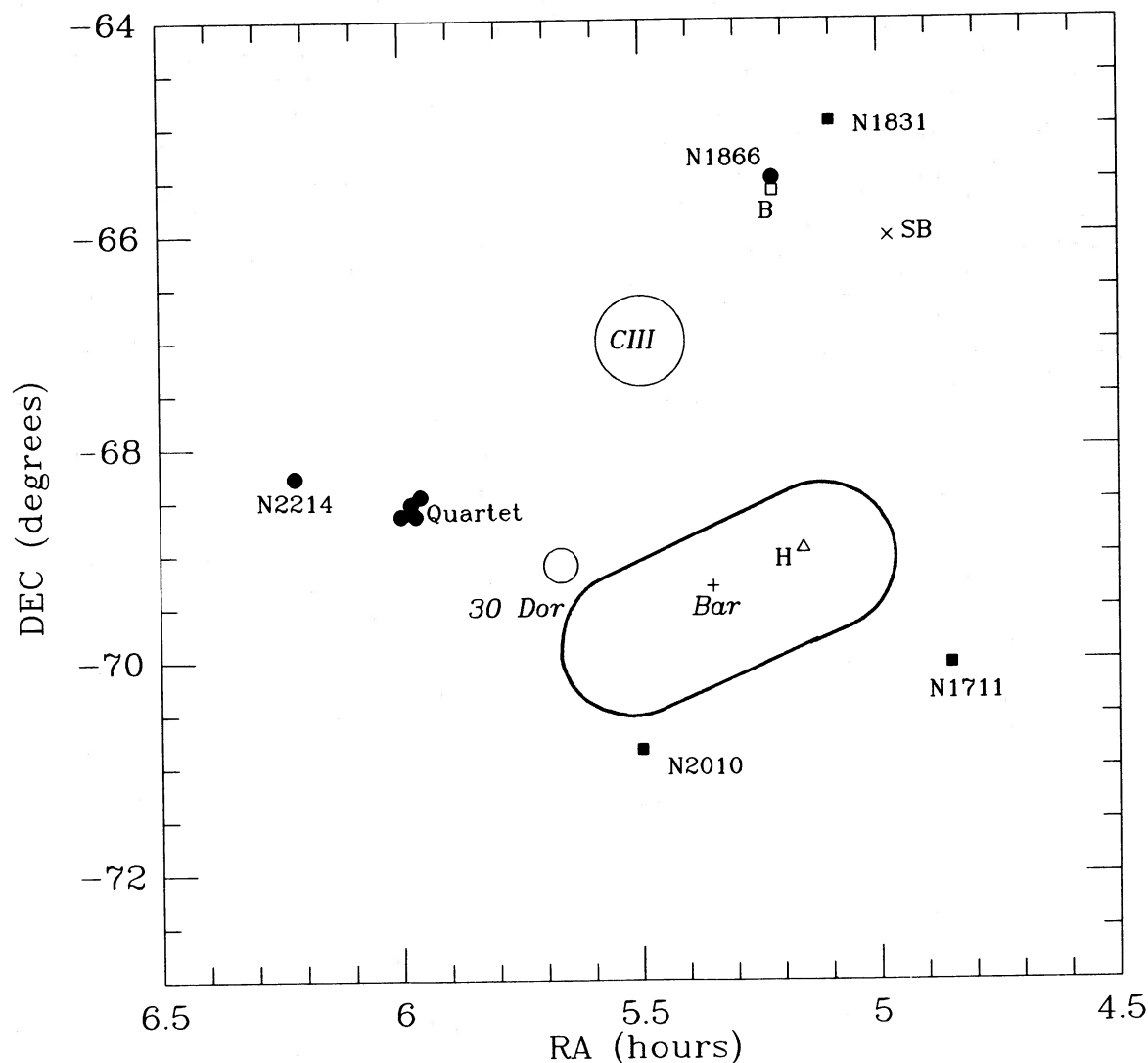


FIG. 1.—Positions on the sky of the clusters in our sample (filled circles) and Mateo's (1988) sample (filled squares), and of the fields for which luminosity functions have been published by Butcher (1977; open square), Stryker and Butcher (1981; cross), Hardy *et al.* (1984; open triangle). The Bar, 30 Dor, Constellation III, and the center of the LMC are also indicated.

time scales. Section VI contains a theoretical discussion of various effects that might have been important during the early evolution of the LMC clusters. In § VII we summarize our conclusions.

II. LUMINOSITY FUNCTIONS

a) Observational Data

The luminosity functions of the six LMC clusters and their surrounding fields were determined from star counts on photographic plates with different limiting magnitudes. They are a byproduct of the work described in Paper I on the structure of the clusters. The star counts give luminosity functions that are inherently cumulative, and we do not attempt to differentiate them. In comparison with CCD images, photographic plates have several well-known disadvantages. However, in the present context, the large area covered by the plates is an important advantage; one can work further out in the clusters where crowding is much less severe and still sample enough

cluster stars that the statistical uncertainties are small. We return to this point in § IV.

Da Costa (1982) used star counts on photographic plates to determine the luminosity functions of three Galactic globular clusters. Two of them, 47 Tuc and NGC 6752, were subsequently observed with CCDs (Harris and Hesser 1985; Penny and Dickens 1986). For NGC 6752, the photographic and CCD results are in excellent agreement. For 47 Tuc, the luminosity functions agree to $V \approx 20$, but at fainter magnitudes they diverge. This discrepancy is probably caused by the nonuniform background, mainly the SMC, across the large 47 Tuc field. The clusters in our sample are easier to study than those in Da Costa's sample because they have much smaller angular sizes and much larger ranges of observable stellar masses.

Our plates of the LMC clusters, all in the B passband, were taken with the 3.9 m Anglo-Australian Telescope and the 1.0 m telescope at Siding Spring Observatory. Typically $\sim 10^3$ stars were counted on each plate. The star counts are described and tabulated in Paper I. In determining the luminosity functions,

we used between four and seven plates for each cluster. The background densities f_b were derived from the counts in regions well outside the clusters (typically at radii between $5'$ and $10'$); these are listed in Table 1. Since the clusters are too young to have lost many stars by evaporation, the surrounding fields should have very little contamination by cluster members. In most cases, the uncertainties in the backgrounds are only 1%, and even in the worst cases, they are only 5%. The backgrounds were subtracted from the total counts in different annuli to determine the radial density of cluster members brighter than the limiting magnitude of each plate.

Most of the star counts are in relatively uncrowded regions of the clusters and the surrounding fields. However, in some cases, particularly near the centers of the clusters, corrections for crowding were appropriate. We followed the standard pro-

cedure of King *et al.* (1968), which was devised specifically for star counts on photographic plates. The corrections depend on the plate scale and the size and density of the faintest stellar images; King *et al.* found an empirical relation between these quantities by comparing plates taken of the same fields with different angular scales, limiting magnitudes, and seeing conditions. The crowding corrections applied to our star counts are listed in Table 7 of Paper I. Only 10% of the counts required corrections of more than 20%, and all counts that required corrections of more than a factor of 2 were excluded. We emphasize that the size of the corrections varies more strongly with radius within a cluster than with the limiting magnitude of the plates, and since we combine counts over large radial ranges, the net effect of the crowding corrections is small even at the faintest magnitudes. We are therefore confident that the luminosity functions derived here are not significantly biased by the corrections we have applied.

The limiting magnitude of each plate was determined by comparisons with photometric sequences from Robertson (1974*b*), Walker (1974), Flower and Hodge (1975), Andersen, Blecha, and Walker (1984), Hodge (1984), and McClure (1987). These are listed in Table 1. The photometry itself is probably accurate to better than 0.2 mag. Although every care was taken to ensure that stars were counted to uniform limits, small variations in the detection threshold are inevitable. As a result, cumulative luminosity functions are more appropriate here than differential ones, which require that all the magnitude intervals be known with high accuracy. We estimate that the total uncertainty in the limiting magnitudes of our plates is less than 0.5 mag. As shown below, such errors do not affect our conclusions.

b) Cluster Luminosity Functions

Since all our plates are in the same passband, we cannot distinguish among stars in different parts of the color-magnitude diagram (CMD). The luminosity functions derived here therefore include both main-sequence and evolved stars. For the following reasons, this does not affect our ability to derive IMFs from the luminosity functions. Figure 2 is a CMD for NGC 1866, from Robertson (1974*b*), which also indicates the limiting magnitudes of our plates. Similar diagrams are available from the literature for all the clusters in our sample. Since the clusters are young, the evolved stars lie along a band of nearly constant B magnitude. Some of the shallowest plates used in Paper I have limiting magnitudes brighter than the faintest evolved stars and we exclude them from the present analysis. This ensures that the limiting magnitude of each plate used to determine the luminosity function corresponds to a unique stellar mass. For example, in the case of NGC 1866 the shallowest plate we use, number 2108, has a limiting magnitude of $B = 17.7$.

We have adopted two different methods to determine the luminosity functions of the clusters. The first is based on the minimum χ^2 fits, described in detail in Paper I, of a model density profile to the star counts on plates with different limiting magnitudes. In addition to the best parameters of the model, this procedure gives the set of multiplicative factors or "shifts" required to bring all the observed profiles for each cluster into as great a coincidence as possible. The shifts, denoted here by f_1 , are therefore measures of the relative numbers of stars in a cluster that are brighter than the limiting magnitudes of the different plates. The values of f_1 are listed in Table 1. (These are related to the shifts defined in the notes to

TABLE 1
CUMULATIVE LUMINOSITY FUNCTIONS

Cluster (1)	Plate (2)	B (3)	$\log f_1$ (4)	$\log f_2$ (5)	$\log f_b$ (6)
NGC 1866.....	529	22.4	2.97	2.86	1.78(0.15)
	878	18.7	2.51	2.53	0.50
	1049	19.6	2.65	2.63	1.04
	1050	18.4	2.25	2.23	0.46
	2108	17.7	2.20	2.14	-0.03
	3467	21.2	2.92	2.87	1.39
NGC 2156.....	539	21.9	2.27	2.30	1.59(0.14)
	1266	17.5	1.40	1.38	-0.02
	1338	22.6	2.33	2.16	1.72
	1339	21.7	2.32	2.27	1.45(0.02)
	1424	18.6	1.80	1.74	0.48
	1729	18.6	1.57	1.67	0.46
	3468	20.7	2.08	2.07	1.15
NGC 2159.....	539	21.9	2.40	2.27	1.61(0.15)
	1266	17.5	1.38	1.35	-0.13
	1338	22.6	2.30	2.29	1.71
	1339	21.7	2.53	2.38	1.44(0.02)
	1424	18.6	1.71	1.69	0.39
	1729	18.6	1.40	1.58	0.48
	3468	20.7	2.00	2.01	1.10
NGC 2164.....	539	21.9	2.40	2.46	1.56(0.13)
	1266	17.5	1.25	1.29	-0.02
	1338	22.6	2.25	2.34	1.74
	1339	21.7	2.15	2.18	1.43(0.01)
	1424	18.6	1.67	1.66	0.54
	1729	18.6	1.50	1.71	0.48
	3468	20.7	2.05	1.98	1.14
NGC 2172.....	539	21.9	2.20	1.84	1.58(0.13)
	1266	17.5	1.20	1.40	-0.02
	1338	22.6	2.05	2.14	1.69
	1424	18.6	1.41	1.53	0.39
	1729	18.6	1.40	1.50	0.41
	3468	20.7	1.70	1.57	1.03
NGC 2214.....	533	22.4	2.73	2.61	1.61(0.01)
	3495	20.4	2.45	2.57	1.08
	3496	19.3	2.44	2.39	0.68
	3497	18.3	2.25	2.19	0.22

NOTES.—Col. (1): cluster name. Col. (2): plate number. Plates with numbers greater than 1500 were taken with the 1 m telescope at Siding Spring Observatory, and the remaining plates were taken with the Anglo-Australian Telescope. Col. (3): apparent limiting B magnitude of plate. Col. (4): relative shifts in the log of the surface density required to construct a composite profile for each cluster, as in Paper I, from star counts on different plates. Col. (5): relative numbers of stars on each plate in a common radial range. Col. (6): background density (number of stars per square arcmin) on each plate. Numbers in brackets are crowding corrections; they are the logarithms of multiplicative factors, and should be added directly to the uncorrected entries.

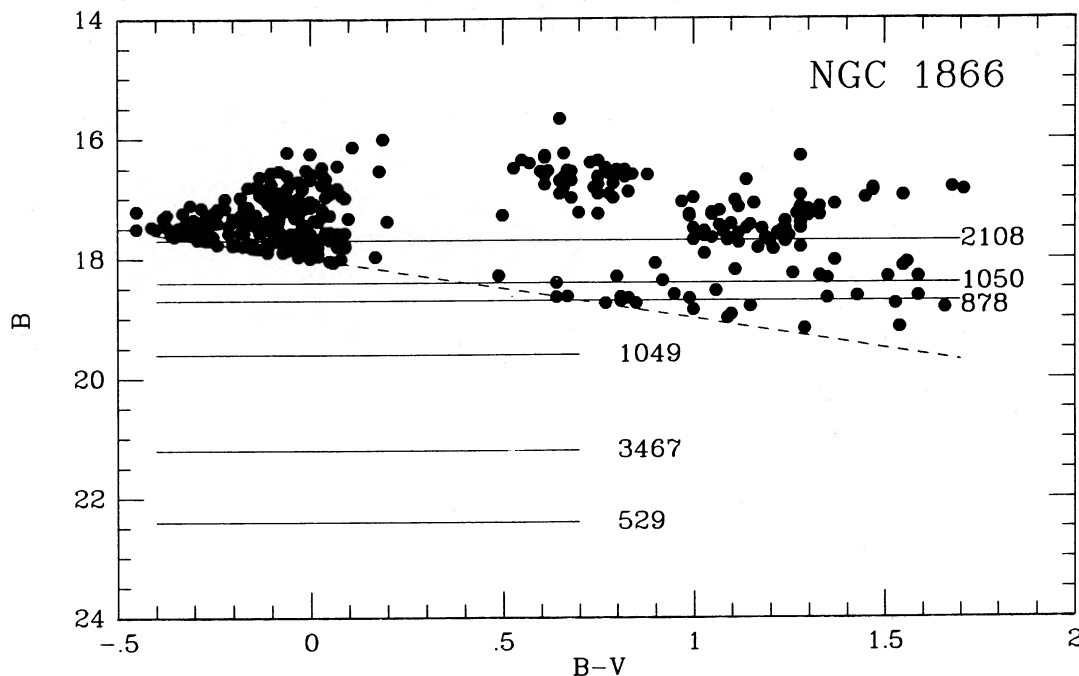


FIG. 2.—Color-magnitude diagram for NGC 1866 from Robertson (1974*b*). The dashed line is the completeness limit of his sample. The solid lines indicate the limiting magnitudes of our plates.

Table 7 of Paper I by $\log f_1 = k - \log f_0$; we have chosen the constant k for each cluster so that the amplitudes of the luminosity functions derived from the two methods are approximately equal.)

In the second method, the luminosity function was simply taken to be the relative number of stars in a common range of radii on plates with different limiting magnitudes. The radial range was chosen for each cluster so as to avoid large corrections for crowding on the deep plates (as specified above) and small extrapolations of the density profiles on shallow plates. Typically, the adopted range was 0.6–3.1, or 10–50 pc. The relative numbers of stars given by this method are denoted by f_2 and are listed in Table 1. We have checked that the luminosity functions are not sensitive to small changes in the adopted radial ranges.

The first method for determining the luminosity functions has the advantage that it makes use of all the star counts on each plate but is less direct in that it forces them to fit a common density profile. While there is no evidence for mass segregation in any of the clusters except perhaps NGC 1866, small variations in the profiles from different plates could be present at a level consistent with the counting statistics and crowding corrections. The second method is more direct in that it uses only the star counts in a common range of radii but has the disadvantage that, since the profiles from deep plates extend to larger radii and those from shallow plates extend to smaller radii, some of the data are not used. As may be seen from Table 1, the results from the two methods are generally in good agreement.

For the three large clusters in our sample, NGC 1866, NGC 2164, and NGC 2214, we have averaged the values of $\log f_1$ and $\log f_2$; these luminosity functions are shown in Figures 3*a*–3*c*. For the three small clusters in the Quartet, NGC 2156, NGC 2159, and NGC 2172, we find no significant differences between the individual luminosity functions. We have com-

pared them by adding the relative numbers of stars f_2 from the second method described above. The composite luminosity function for the three small clusters is shown in Figure 3*d*. The vertical error bars shown in Figures 3*a*–3*d* are the sum of the crowding corrections and the $N^{1/2}$ counting errors; as a result, they are probably larger than the true uncertainties. Since we have plotted cumulative luminosity functions, the errors at different magnitudes are not independent and are therefore used only as a rough guide in fitting the models described below.

c) Field Luminosity Functions

The luminosity functions of the fields surrounding the clusters in our sample were derived from the background densities listed in Table 1. We have plotted in Figure 4*a* the four independent determinations in the vicinity of the Quartet (after excluding regions that might be contaminated by neighboring clusters). The agreement between the luminosity functions is excellent. The dashed curve shows the mean relation. In Figure 4*b*, we have plotted the luminosity functions for the fields surrounding the other two clusters in our sample, NGC 1866 and NGC 2214. They are similar to the luminosity functions of the fields near the Quartet. However, the luminosity functions of all the fields are significantly steeper than those of the clusters in our sample, since the fields contain stars with a much wider range of ages than do the clusters.

Luminosity functions for several other fields in the LMC have been published or can be derived from data in the literature. Butcher (1977) studied a region just south of NGC 1866, which can be used as a check on our results. We derived a cumulative luminosity function from his color-magnitude diagram by counting all stars down to different limiting B magnitudes. As Figure 4*c* shows, the agreement between the luminosity functions derived from our data and Butcher's data is good, including the absolute normalization (number per

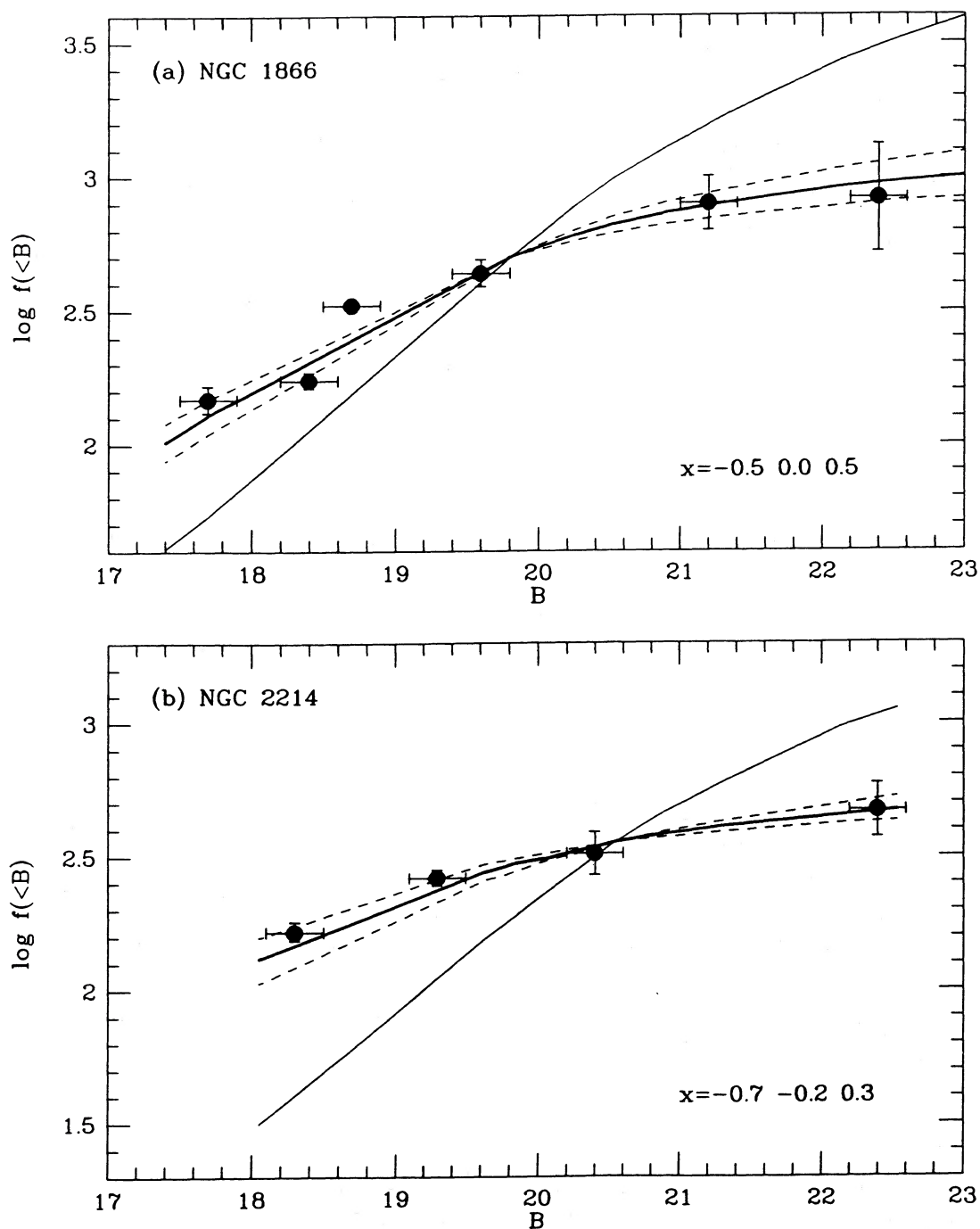


FIG. 3.—(a–d) Cumulative luminosity functions for the LMC clusters in our sample, derived as described in § IIb and listed in Table 1. An arbitrary normalization has been applied. The vertical error bars are the sum of the crowding corrections and the $N^{1/2}$ errors; the horizontal error bars represent the accuracy of the photometry used to derive the limiting magnitudes of the plates. The solid and the dashed curves are for power-law IMFs, calculated from eq. (1) with the values of x indicated. The steep solid curves show a model with $x = 2.5$

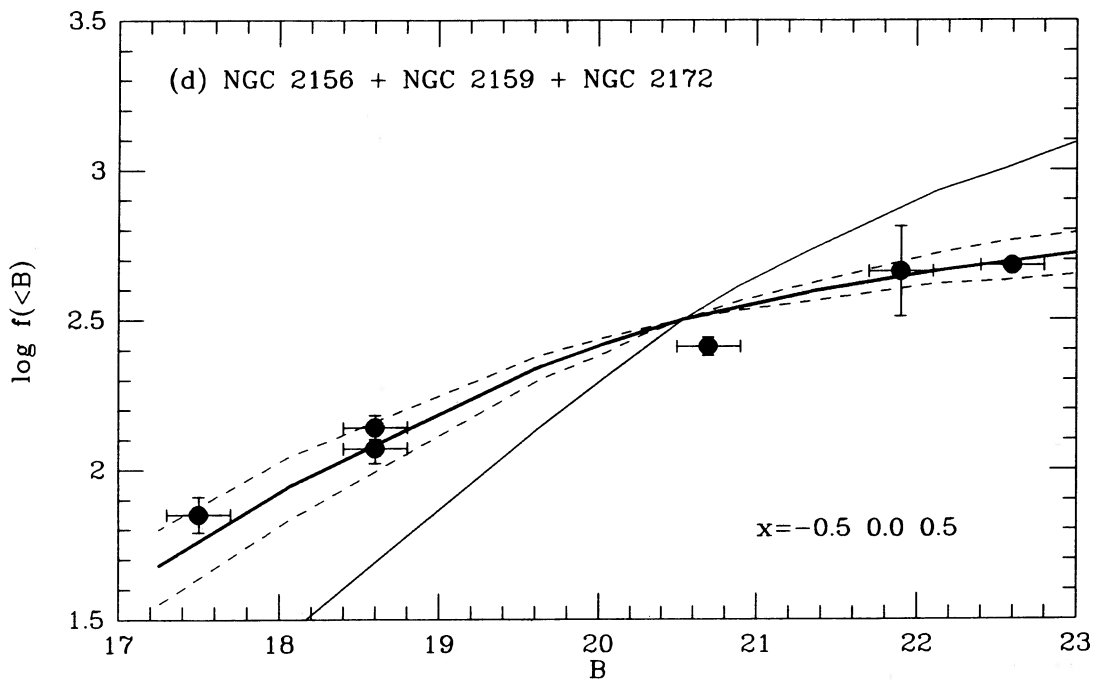
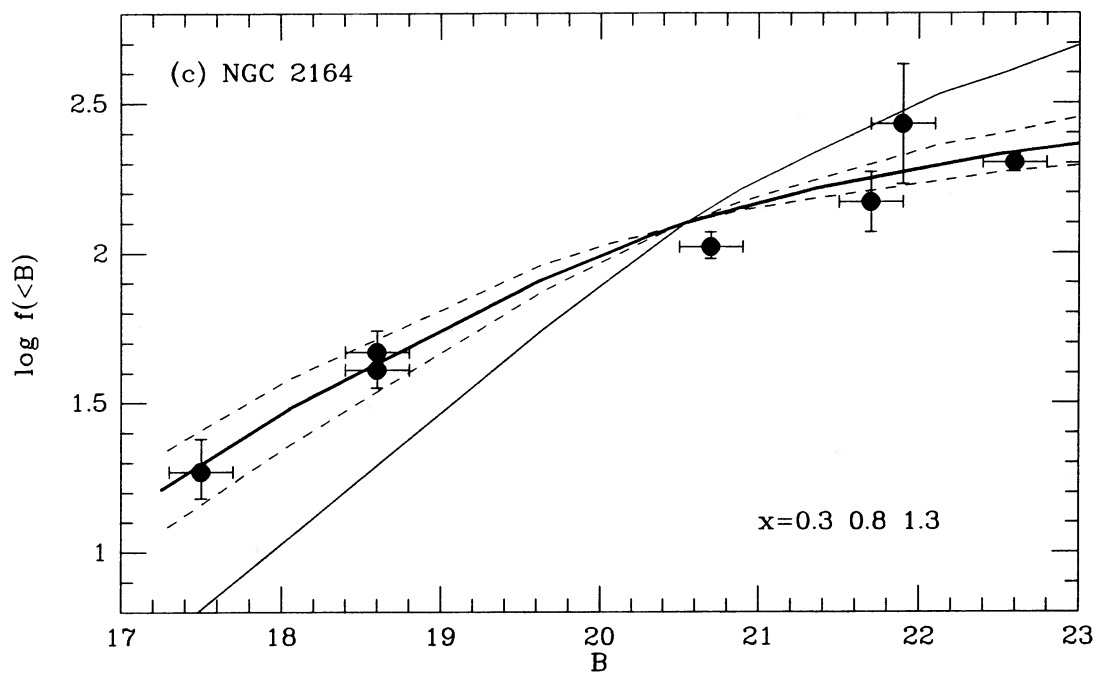


FIG. 3—Continued

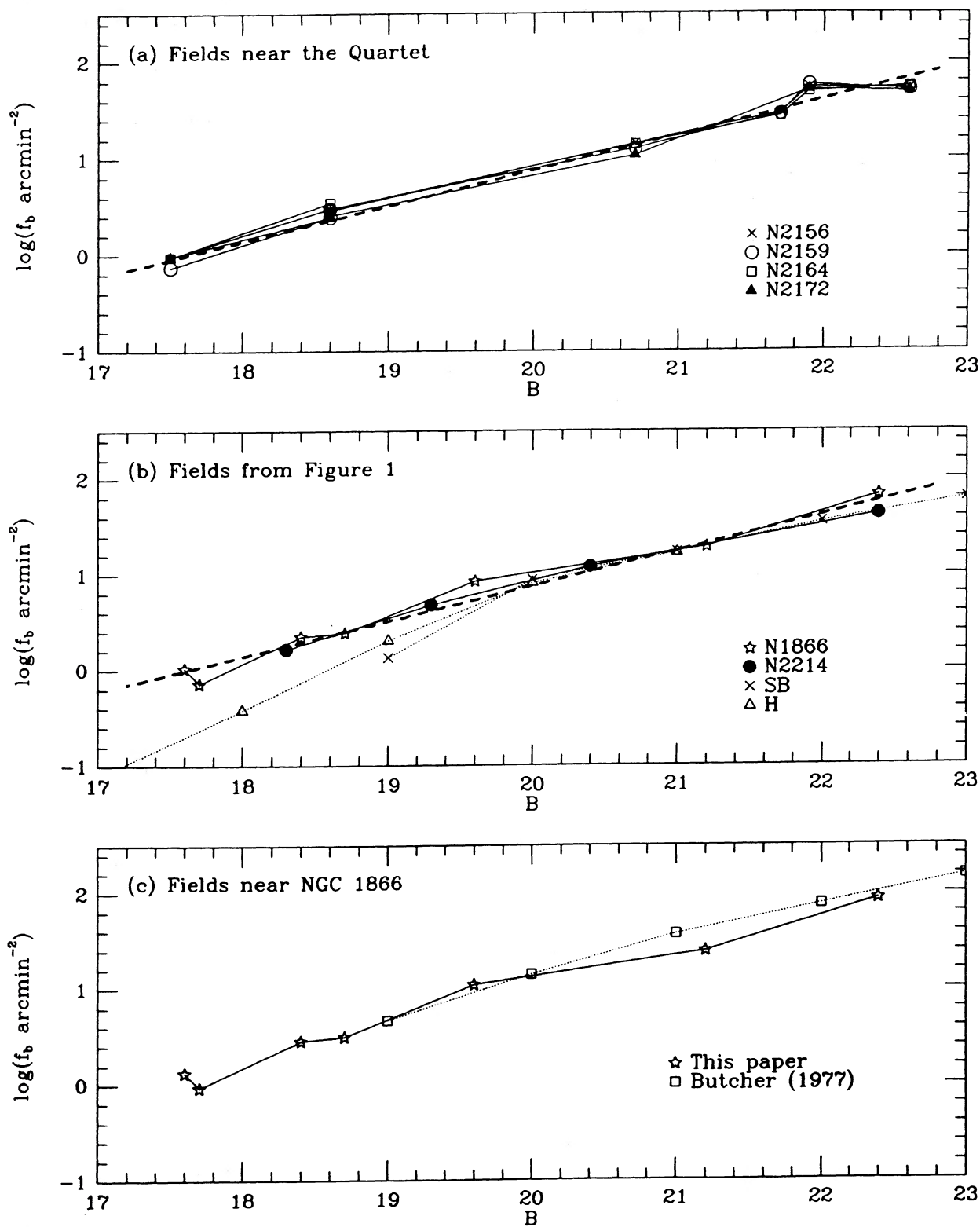


FIG. 4.—(a-c) Cumulative luminosity functions for (a) the field surrounding the clusters in the Quartet, (b) fields surrounding NGC 1866, NGC 2214, near NGC 1783, and in the Bar NW. The latter two are discussed in § IIc. The dashed line is the mean relation for the Quartet and is the same as in (a). (c) Cumulative luminosity functions for the field surrounding NGC 1866 from this paper and from Butcher (1977). The latter is derived as described in the text. The curves in (a) and (c) reflect the true stellar densities; in (b) the curves have been arbitrarily normalized to coincide at $B = 21$.

square arcmin). Stryker and Butcher (1981) studied a field near NGC 1783, and Hardy *et al.* (1984) studied one at the north-west end of the bar of the LMC. (These are indicated by the symbols SB and H in Fig. 1.) The cumulative luminosity functions are plotted in Figure 4*b*. In this case, the curves have been arbitrarily normalized at $B = 21$. Two other determinations of the luminosity functions of fields in the LMC by Flower *et al.* (1980) and Brück (1984) lie between those shown in Figure 4*b*.

The field luminosity functions of the different regions are all similar at faint magnitudes while the proportion of bright stars varies markedly. These differences may reflect local variations in either the IMF or the star formation rate or both. Since it is quite likely that the star formation rate does vary on small spatial and temporal scales, but in ways that would be difficult to measure or predict, we do not attempt to derive IMFs for any of the fields discussed here. We emphasize that the variations at the bright ends of the luminosity functions shown in Figure 4*b* do not contradict the evidence from several nearby galaxies that luminosity functions are "universal" when averaged on much larger scales (Freedman 1985; Scalo 1986).

III. MASS FUNCTIONS

a) Stellar Models

To derive IMFs from the luminosity functions, we need the ages of the clusters, and the stellar mass corresponding to the limiting magnitude of each plate. We can obtain these quantities from stellar evolution models and published color-magnitude diagrams. As discussed in § II*b*, the limiting magnitudes of all our plates are deeper than the faintest evolved stars. Thus, in the derivation of cumulative IMFs, we only need to know the mass-luminosity relation for main-sequence stars. The relevant metallicity in such comparisons is $Z \approx 0.01$. The reddening of the clusters is taken to be $E(B - V) = 0.10 \pm 0.03$ (Persson *et al.* 1983), and the distance modulus of the LMC to be 18.6 (Sandage and Tammann 1974). It has been suggested that the true distance modulus may be as small as 18.2 (Schommer, Olszewski, and Aaronson 1984; Chiosi and Pigatto 1986; Conti, Garmany, and Massey 1986); as discussed below, the effect on our results of adopting this smaller value is negligible.

VandenBerg (1985) gives a critical comparison of recent stellar evolution models. For stars with masses in the range $0.7 \leq m/M_{\odot} \leq 3.0$, we adopt his models, which are calculated for $Y = 0.25$ and $Z = 0.01$. For more massive stars, we use the models of Becker (1981), which are calculated for $Y = 0.28$ and $Z = 0.01$. VandenBerg tabulates tracks in the observational plane, while Becker's are given only in the theoretical plane. We have therefore converted Becker's models to the observational plane using the same color-temperature relation and bolometric corrections as adopted by VandenBerg. Figure 5*a* shows the absolute magnitude M_B plotted against age for the two sets of models. The only overlap is for the $3 M_{\odot}$ star, and in this case the agreement is excellent. Figure 5*b* shows M_B plotted against $B - V$ for the $3 M_{\odot}$ star. Becker's track is bluer near the turnoff than VandenBerg's, and the evolved branch is brighter. However, for a given mass, the ages along Becker's track are also systematically smaller, and the two offsets conspire so that the relation between M_B and age along the evolved branch is the same for both sets of models. Finally, Figure 5*c* shows the stellar mass-luminosity relation for $Z = 0.01$ and four different ages. The zero-age main sequences (ZAMSs) for $Z = 0.006$ and 0.0169 , from VandenBerg and

Bridges (1984), are also shown. The similarity between the solar abundance curve, which spans the full range of masses, and that for $\log(\tau/\text{yr}) = 7.2$, which is a composite of VandenBerg's (1985, hereafter VdB) and Becker's (1981) models, gives us confidence that combining the two sets of models has not introduced systematic errors into the mass-luminosity relation. The dashed curve in Figure 5*c* is for a solar abundance model that includes convective overshooting (Bertelli *et al.* 1986). It is very similar to the model without overshooting.

To determine the turnoff masses and ages of the clusters, we use the CMDs published by Robertson (1974*b*), and Flower and Hodge (1975). Those for the clusters in the Quartet are quite similar, and a composite CMD was therefore constructed. Each CMD contains 100–350 stars down to $B \approx 18$. The turnoff masses m_t were derived from Becker's stellar tracks but corrected for the offset shown in Figure 5*b*, by $\log m_t(\text{VdB}) = \log m_t(\text{Becker}) + 0.04$. The adopted values of m_t are listed in Table 2 and have uncertainties of $\pm 0.5 M_{\odot}$. The ages of the clusters were also determined from a comparison with Becker's models. Because, as described above, the difference in luminosity is offset by a difference in age, no correction to the inferred ages is needed. Our adopted values of $\log(\tau/\text{yr})$ are listed in Table 2; they agree with previous estimates to within ± 0.1 . Finally, the solid curves in Figure 5*c* were used to convert the limiting magnitude of each plate to a limiting mass.

b) Cluster Mass Functions

We now determine what IMFs are compatible with the luminosity functions derived above. We adopt the usual definition that $\phi(m)dm$ is the number of stars born in the mass range $(m, m + dm)$, and we consider power-law models of the form $\phi(m) \propto m^{-(1+x)}$. In this notation the Salpeter IMF has $x = 1.35$. For a given value of the slope x , the "predicted" luminosity function is then

$$f(<B) \propto \int_{m(B)}^{m_t(\tau)} dmm^{-(1+x)}, \tag{1}$$

where $m_t(\tau)$ is the turnoff mass of a cluster with an age τ , and $m(B)$ is the mass-luminosity relation from Figure 5*c*. The models were calculated for a range of x and fitted by eye to the luminosity functions as shown in Figures 3*a*–3*d*. The IMF slopes for the dotted curves differ from those of the best fitting solid curves by ± 0.5 . For the young clusters in our sample, changes of $\pm 0.5 M_{\odot}$ in the turnoff mass do not affect the

TABLE 2
PARAMETERS DERIVED FROM STELLAR EVOLUTION MODELS

Cluster (1)	$\log(\tau/\text{yr})$ (2)	m/M_{\odot} (3)	m_t/M_{\odot} (4)	x (5)
NGC 1866.....	7.7	1.5–5.1	6.1	0.0
NGC 2164.....	7.5	1.4–5.8	7.7	0.8
NGC 2214.....	7.5	1.5–4.7	7.7	-0.2
NGC 2156 }.....	7.5	same as NGC 2159		0.5
NGC 2159 }.....		1.4–5.8	7.7	
NGC 2172 }.....		same as NGC 2159		

NOTES.—Col. (1): cluster name. Col. (2): cluster age, estimated using isochrones described in § III, and CMDs from Robertson (1974*b*), and Flower and Hodge (1975). Col. (3): range of stellar masses corresponding to the limiting magnitudes of the plates in Table 1. Col. (4): turnoff mass; uncertainties are $\pm 0.5 M_{\odot}$. Col. (5): slope of the IMF, derived as described in the text. The uncertainties estimated by eye from Figs. 3*a*–3*d* are ± 0.5 .

1989ApJ...336..734E

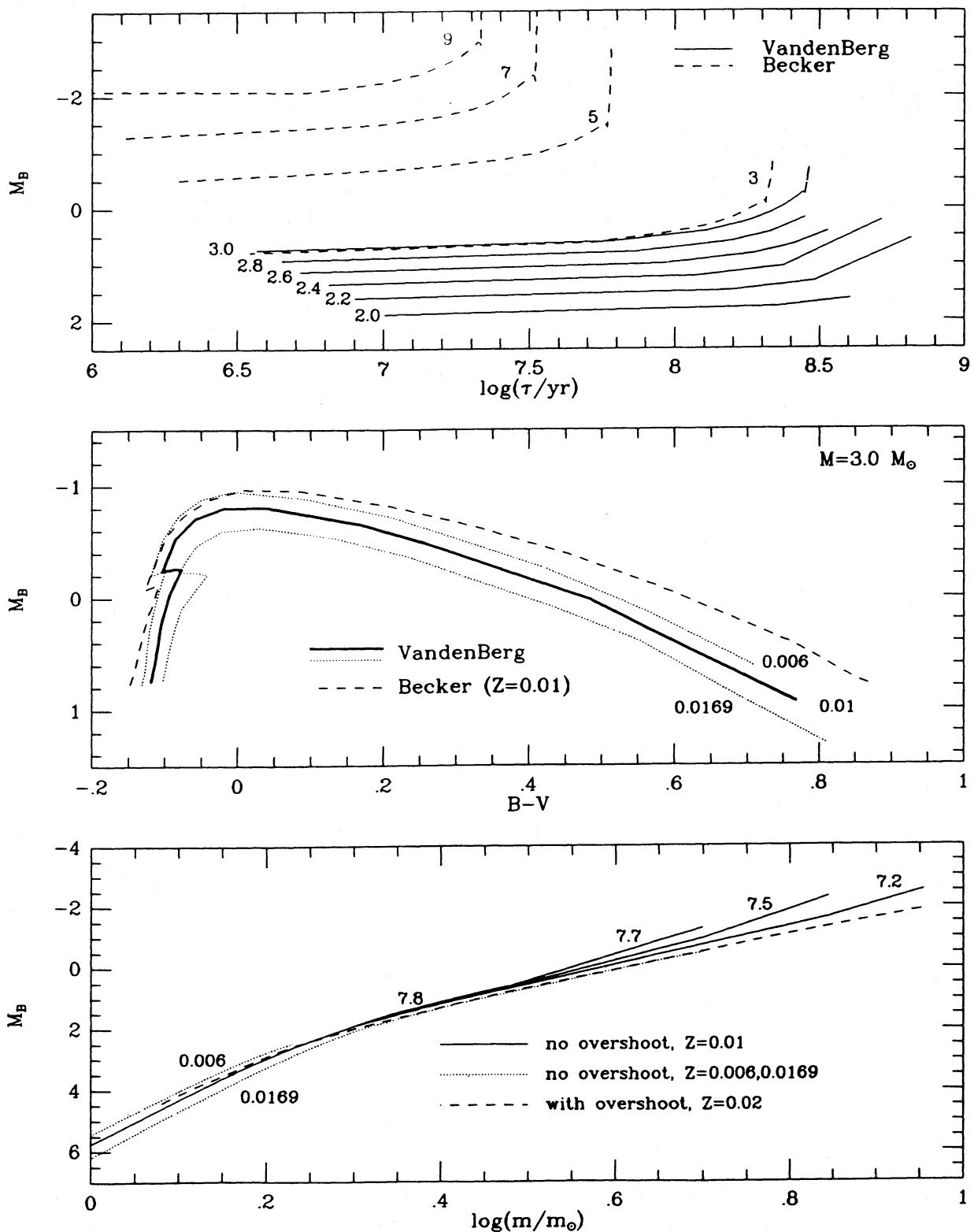


FIG. 5.—(a-c) Stellar evolution tracks used in converting luminosity functions to mass functions. (a) Absolute magnitude plotted against age for models from Vandenberg (1985; solid curves) and Becker (1981; dashed curves) for the stellar masses indicated. (b) Stellar tracks for a $3 M_\odot$ star from Vandenberg (1985) for the metallicities indicated (solid and dotted curves), and from Becker (1981; dashed curve). (c) Main-sequence mass-luminosity relation for the same models as in (a) and (b), for the values of $\log(\tau/\text{yr})$ indicated. The dotted curves are the ZAMS for the values of Z indicated, and are from Vandenberg and Bridges (1984). The dashed curve is the ZAMS with convective overshooting from Bertelli *et al.* (1986).

inferred x values significantly. As the IMF steepens, the difference between the predicted and the observed luminosity functions becomes very large. This is illustrated in Figures 3a–3d, where we also show models calculated with $x = 2.5$ for each cluster.

We find that the IMFs of the clusters are remarkably flat for stellar masses between 1.5 and $6 M_{\odot}$. The best fitting slopes are in the range $-0.2 \lesssim x \lesssim 0.8$ and are listed in Table 2. There is some evidence that x varies from one cluster to another, but the uncertainties are such that a common IMF slope for all the clusters cannot be ruled out. Our results supersede those of Freeman (1977), who derived IMFs for the same clusters. The differences between his x values and those found here are due mainly to the use of more recent stellar models and bolometric corrections in the mass-luminosity relation.

To test the sensitivity of the IMF slope to the adopted stellar models, we have repeated the above procedure using tracks with different metallicities and with convective overshooting. Variations in metallicity within the range of models plotted in Figure 5c change x by only ± 0.1 . Including convective overshooting decreases x by $\lesssim 0.1$. Finally, adopting a distance modulus of 18.2 instead of 18.6 increases the best fitting x values by $\lesssim 0.3$. All of these are within the estimated uncertainties due to counting statistics and crowding corrections. If the limiting magnitudes of all the shallower plates were systematically too bright by 0.5–1.0 mag, while those for all the deeper plates were too faint by the same amount, then x would have been underestimated by ≈ 0.5 . Such a conspiracy seems unlikely.

IV. COMPARISON WITH OTHER CLUSTER IMFs

a) LMC Clusters

Mateo (1988) has made a thorough study of the stellar content of six rich clusters in the Magellanic Clouds, from CCD observations in the B and V passbands. He uses the colors to identify the evolved stars at each magnitude and hence to determine main-sequence luminosity functions in differential form. These are converted to IMFs through mass-luminosity relations from the same stellar evolution models as we have used. Mateo finds that the IMFs of all the clusters in his sample are similar to each other but much steeper than the IMFs we have found. The slope is $x \approx 2$ for stars more massive than $3 M_{\odot}$ and $x \approx 3$ for less massive stars; over the full range of masses, 1 – $10 M_{\odot}$, the best fitting slope is $x \approx 2.5$. The IMFs of the clusters in Mateo's sample are derived typically at radii from $0'$ to $1'3$, where the density of faint stellar images is high. As Mateo acknowledges, the main uncertainty in his results is due to the large corrections for crowding and incompleteness that he is forced to make. The corrections are usually less than a factor of 2 at bright magnitudes ($B \lesssim 20$) but rise to factors between 2 and 10 at faint magnitudes ($B \gtrsim 22$).

Unfortunately, a definitive comparison between Mateo's results and ours is not possible at this time. We do, however, have star counts for one of the clusters in his sample, NGC 1831. This cluster was not included in our original study because it is relatively old ($\tau \approx 2 \times 10^8$ yr) and the observable range of stellar masses is not large enough for us to determine a reliable IMF slope. The open circles in Figure 6a show the cumulative luminosity function derived from the star counts over the same range of radii as was used by Mateo ($0'6$ – $1'6$). For comparison with our results, Mateo has kindly provided enough information for us to derive a cumulative luminosity

function for NGC 1831 from his data, that includes evolved stars. This is shown by the filled circles in Figure 6a. The agreement between the two luminosity functions is satisfactory but the comparison depends heavily on the star counts on a single plate. At magnitudes fainter than $B \approx 21$, the corrections for incompleteness in both Mateo's and our luminosity functions become large and a comparison would not be meaningful. As we have already noted, the luminosity functions for the other clusters in our sample were determined at much larger radii where the corrections for crowding are small even at $B \approx 22.5$.

We now demonstrate that there are no significant differences between the IMF slopes derived from the luminosity function in cumulative and differential forms. For this purpose, we use Mateo's luminosity function for NGC 1831, which is plotted in Figure 6b over the range of magnitudes, $19 \lesssim B \lesssim 23$. The solid and dashed curves show models calculated with a turnoff mass of $m_t = 3.3 M_{\odot}$ and IMF slopes of $x = 2.0, 2.5$, and 3.0 . We have used the same procedure as the one described in § IIIb for the clusters in our sample. The dotted curves in Figure 6b were calculated for $x = 2.5$ with $m_t = 3.2$ and $3.4 M_{\odot}$. They show that small variations in the turnoff mass have little effect on the model luminosity functions except near the turnoff. The IMF slope that best fits the cumulative luminosity function, $x = 2.5$, agrees well with the value $x = 3.0 \pm 0.7$ derived by Mateo from the differential luminosity function.

We conclude that neither differences in the luminosity functions nor in the methods used to derive IMFs from them appears to account for the discrepancies between the x values found by Mateo and those found in the present study. The comparison is, however, quite limited. If both Mateo's and our results are correct, then there appear to be significant variations in the IMFs from one cluster to another. In this connection, it is worth noting that the ages and locations of the clusters in the two samples are different. One of the clusters Mateo has studied is in the SMC, and of the five in the LMC, three are older than the clusters we have studied. The other two clusters in Mateo's sample, NGC 1711 and NGC 2010, are nearer the Bar, in denser regions of the LMC than our clusters (see Fig. 1). It is possible that the IMFs of the clusters depend on some combination of their ages and environments. Clearly, further observations are needed to resolve these issues.

b) Galactic Open Clusters

The stellar content of open clusters in the Milky Way has been studied by several authors, and there have been contradictory claims concerning variations in the IMFs. Because Galactic open clusters are relatively poor, the approach has generally been to combine data from many clusters in order to reduce the statistical uncertainties. The results are reviewed by Scalo (1986). He concludes that there is no strong basis for rejecting the hypothesis that the IMF is "universal," with a slope $x \approx 1.5 \pm 0.2$ for $m \gtrsim 1 M_{\odot}$. However, even fairly large variations from one cluster to another cannot be ruled out. There is some evidence that the IMFs are flatter in larger clusters (Burki 1977).

Ideally we would like to compare the IMFs of the young LMC clusters in our sample with those of Galactic open clusters of similar age, derived using the same method as for the LMC clusters. The pair of clusters h and χ Per, at a distance of ~ 2 kpc, have ages of 1 – 2×10^7 yr, and masses of $\sim 4 \times 10^3 M_{\odot}$ (Vogt 1971). Thus they are less massive but only slightly younger than the clusters in our sample. Figure 7 shows the

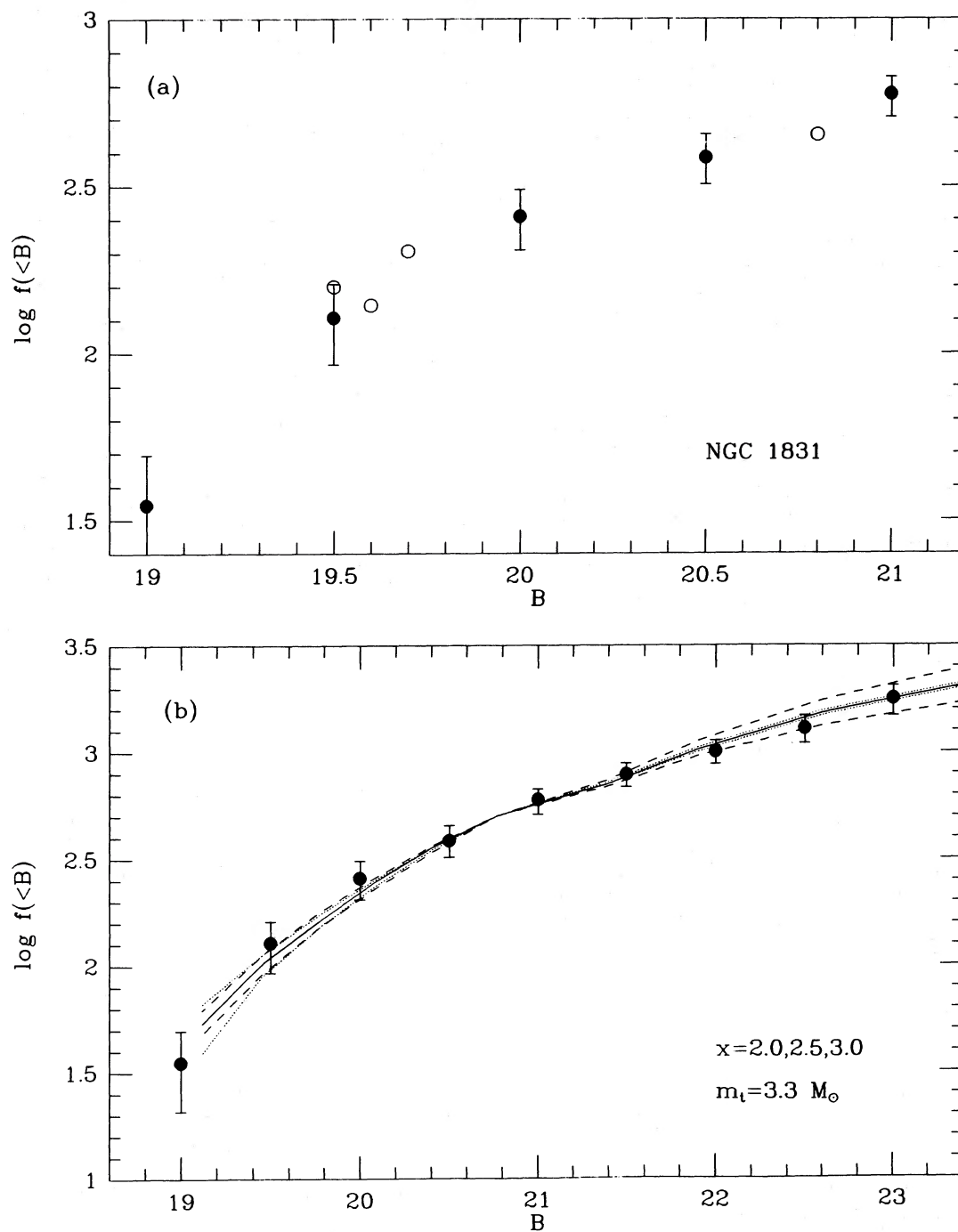


FIG. 6.—(a–b) Cumulative luminosity functions for NGC 1831 derived from Mateo's (1988) data (*filled symbols*), and our data (*open symbols*). Both of these include evolved stars. The error bars represent $N^{1/2}$ statistical uncertainties but not crowding corrections. (a) Comparison of our data with Mateo's over the range of magnitudes where corrections for crowding and incompleteness are less than a factor of 2. (b) Fits of our models to Mateo's data over the full range of magnitudes. The solid and dashed curves are for $m_t = 3.3 M_\odot$ and $x = 2.0, 2.5,$ and 3.0 . The dotted curves are for $x = 2.5$ and $m_t = 3.2 M_\odot$ and $m_t = 3.4 M_\odot$.

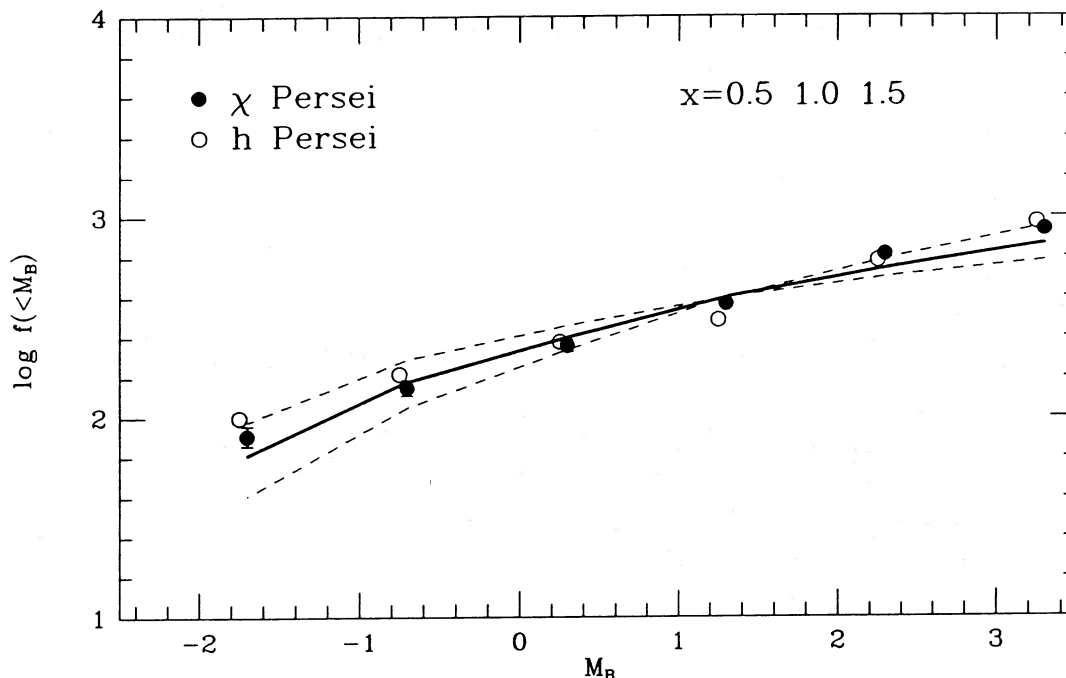


FIG. 7.—Cumulative luminosity functions for the Galactic open clusters h and χ Per. These were calculated in the same way as for the LMC clusters, with the values of the IMF slope indicated, and $m_l = 15 M_\odot$. The error bars represent $N^{1/2}$ uncertainties.

luminosity functions for h and χ Per, constructed by counting stars in bins of constant B magnitude in the CMDs from Vogt (1971). The luminosity function for each cluster includes ~ 900 stars. Superposed on the data are models calculated with the mass-luminosity relation from Figure 5c. We find that the luminosity functions for h and χ Per correspond to IMFs with $x \approx 1.0 \pm 0.5$ over the mass range $1.5 \lesssim m/M_\odot \lesssim 8.5$.

c) Galactic Globular Clusters

The observable range of stellar masses in Galactic globular clusters, $0.4\text{--}0.8 M_\odot$, does not overlap with that in the young LMC clusters, but the results may be compared if we assume that massive stars formed in globular clusters with the same IMF slope as stars with lower masses. McClure *et al.* (1986) studied the luminosity functions of nine Galactic globular clusters and found that the corresponding IMFs had slopes in the range $-0.5 \lesssim x \lesssim 2.5$. As the result of mass segregation, there is some uncertainty as to whether the observed luminosity functions are representative of the overall stellar content of the clusters. Moreover, the IMFs depend on the assumed mass-luminosity relation which, for metal-poor stars, is controversial (D'Antona 1987).

McClure *et al.* (1986) found a correlation between the IMF slopes and metallicities of Galactic globular clusters in the sense that the more metal rich clusters have flatter IMFs. The young LMC clusters have metallicities $\approx 0.5 Z_\odot$ (Cohen 1982; Becker and Mathews 1983; Becker, Mathews, and Brunish 1984; Schommer and Geisler 1988). Thus, if their IMFs are generally as flat as those derived here, they would follow the trend found by McClure *et al.* However, if the steep IMFs derived by Mateo are more representative, this would not be the case. As will be shown in the next section, the mass-to-light ratio increases dramatically with age in a cluster with a flat IMF, due to the accumulation of dark remnants from the abundant high-mass stars (see Figs. 8a and 8b). This is in con-

trast with the behavior of populations with steep IMFs. As noted by Elson and Freeman (1985), the old LMC clusters appear to have mass-to-light ratios lower than those predicted for standard IMFs. This suggests that the old LMC clusters may have been born with much steeper IMFs than the young clusters. Since the old clusters are more metal poor, this might be indirect evidence that the correlation between IMF slope and metallicity is also present in the LMC.

V. MASS-TO-LIGHT RATIOS AND RELATED PARAMETERS

In Paper I we estimated the total masses of 10 young clusters in the LMC, including those discussed here, using mass-to-light ratios from stellar population models with IMF slopes in the range $1.1 \lesssim x \lesssim 2.2$. Since the IMFs now appear to be flatter, the values of M/L should be lower than our previous estimates. In a subsequent paper, we set limits on the mass-to-light ratios of three of these clusters from direct measurements of their velocity dispersions (Lupton *et al.* 1988). Here we use stellar population models from Yamanaka (1987), which are based on the new Yale isochrones and are calculated for $Z = 0.01$ and $Y = 0.30$. The IMF is assumed to be a single power law with sharp cutoffs:

$$\phi(m) = \begin{cases} Am^{-(1+x)} & \text{for } m_l < m < m_u; \\ 0 & \text{otherwise.} \end{cases} \quad (2)$$

Two values were adopted for the lower mass cutoff: $m_l = 0.10$ and $0.25 M_\odot$. With flat IMFs, the exact value of m_l is not important for most of the results presented below. The choice of upper cutoff can, however, affect the results significantly; we adopt $m_u = 35$ and $100 M_\odot$. These are consistent with the range suggested by observations of the most massive stars in very young clusters and associations in the Milky Way and the LMC (Lucke 1974; Humphreys and McElroy 1984; Melnick

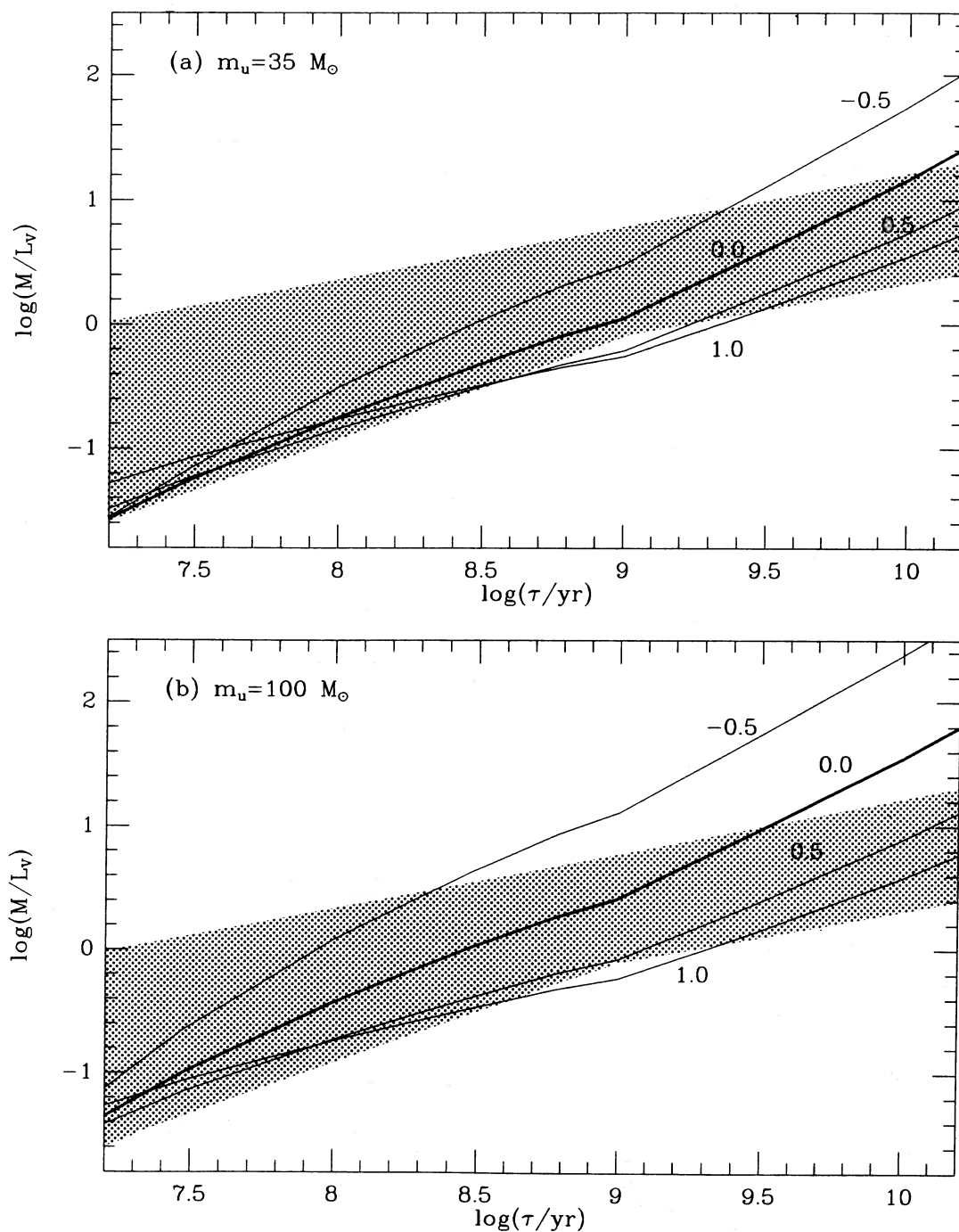


FIG. 8.—(a–b) Mass-to-light ratio plotted against age from the stellar population models of Yamanaka (1987), for power-law IMFs with the slopes indicated. The models were calculated for $Z = 0.01$, $m_l = 0.25 M_\odot$, and (a) $m_u = 35 M_\odot$ and (b) $m_u = 100 M_\odot$. For the range of x values shown, variations in m_l do not affect the mass-to-light ratios significantly. The shaded regions show the range of M/L ratios considered in Paper I.

TABLE 3
PARAMETERS DERIVED FROM STELLAR POPULATION MODELS

Cluster	$\log (M/L_V)$ (M_\odot/L_\odot)	$\log M_\infty$ (M_\odot)	$\log \rho_0$ ($M_\odot \text{ pc}^{-3}$)	σ_0 (km s^{-1})	$\log r_t$ (arcsec)	$\log \tau_c(r_h)$ (yr)	$\log \tau_r(0)$ (yr)
NGC 1866.....	-1.07 to -0.35	4.9-5.7	1.6-2.3	2.1-4.8	2.3-2.7	6.7-7.1	8.9-9.3
NGC 2156.....	-1.25 to -0.95	3.8-4.1	1.8-2.1	1.1-1.5	2.0-2.3	6.6-6.8	7.9-8.1
NGC 2159.....	-1.25 to -0.95	4.3-4.6	1.6-1.9	0.9-1.3	1.9-2.2	6.0-7.2	7.9-8.1
NGC 2164.....	-1.24 to -0.90	4.3-4.6	2.1-2.4	1.6-2.4	2.2-2.5	6.5-6.7	8.2-8.4
NGC 2172.....	-1.25 to -0.95	3.6-3.9	1.4-1.7	0.8-1.1	1.9-2.2	6.7-6.9	8.1-8.3
NGC 2214.....	-1.25 to -0.50	4.3-5.1	1.4-2.2	1.1-2.6	2.1-2.6	6.9-7.3	8.2-8.6

NOTES.—Col. (1): cluster name. Col. (2): range in mass-to-light ratio from the stellar population models of Yamanaka 1987; see Figs. 8a and 8b. Col. (3): total mass estimated from M/L_V in col. (2), and the asymptotic luminosity L_∞ from Paper I. Col. (4): central density. Col. (5): central velocity dispersion in one dimension, derived from the equation of hydrostatic equilibrium as in Paper I. Cols. (6)–(8): eventual tidal radius, crossing time at the median radius, and central relaxation time, calculated as in Paper I.

1985). There is, however, some evidence that 30 Dor contains stars with masses exceeding $200 M_\odot$ (Walborn 1984).

The mass of a cluster of age τ is given by

$$M(\tau) = A \int_{m_l}^{m_t(\tau)} dm m^{-x} + A \int_{m_t(\tau)}^{m_u} dm w(m) m^{-(1+x)}, \quad (3)$$

where $w(m)$ is the mass of the remnant produced by a star with an initial mass m . We adopt the relation

$$w(m) = 0.38 M_\odot + 0.15m \quad (4)$$

(Iben and Renzini 1983), which should be accurate for white dwarfs but may overestimate the masses of neutron stars and black holes. We have also calculated the total mass using equation (4) for $m \leq 6.8 M_\odot$ and $w(m) = 1.4 M_\odot$ for $m > 6.8 M_\odot$. This has the effect of decreasing $\log (M/M_\odot)$ by 0.4 for $x \approx 0$ and by 0.2 for $x \approx 0.5$. For $x \geq 1$, the effect is negligible.

Figures 8a and b show M/L_V plotted against age for the range of IMF slopes determined here. The mass-to-light ratio increases more rapidly with age for smaller x values as a result of the larger numbers of remnants. The range in M/L_V predicted for each cluster is listed in Table 3. These estimates are consistent with the upper limits derived from direct measurements of the internal velocities of stars in three of the clusters. (Lupton *et al.* 1988). Here we use the new mass-to-light ratios, derived from the stellar population models, to revise our estimates from Paper I of the total masses M_∞ , central densities ρ_0 , and central velocity dispersions σ_0 ; the new values are listed in Table 3. The masses range from 4×10^3 to $5 \times 10^5 M_\odot$, the central densities from 25 to $250 M_\odot \text{ pc}^{-3}$, and the central velocity dispersions from 1 to 5 km s^{-1} . The lower limits on M_∞ , ρ_0 , and σ_0 are close to those estimated in Paper I, whereas the upper limits are significantly smaller than our previous estimates. The central densities and velocity dispersions depend on the core radii, which are uncertain for the three smallest clusters. The total masses, however, are independent of the core radii. Also listed in Table 3 are revised estimates of the crossing times $\tau_c(r_h)$, central relaxation times $\tau_r(0)$, and eventual tidal radii r_t , of the clusters. These reinforce our conclusions from Paper I that the clusters in our sample are dynamically well mixed, but not relaxed by two-body encounters, and that they overflow the boundaries set by the tidal field of the LMC.

VI. EARLY EVOLUTION OF THE CLUSTERS

Our observational results suggest that at least some of the rich young clusters in the LMC have mass functions that are

remarkably flat over the range $1.5 \lesssim m/M_\odot \lesssim 6$. If the IMFs had similar slopes above the present turnoffs, the protoclusters would have contained a large proportion of very massive stars, and stellar winds, supernovae, and other stellar ejecta would have been important. We consider each of these effects in turn. Because the time scales for star formation, gas removal, and the dynamical response of the clusters are of the same order of magnitude, the different processes may combine in ways that are difficult to predict. Thus only a very rough treatment is justified at this stage of our understanding. The quantities calculated below are based on an IMF with a single power law and sharp cutoffs at $m_l = 0.1$ or $0.25 M_\odot$, and $m_u = 35$ or $100 M_\odot$, as before. The coefficient of proportionality, A , is generally eliminated in favor of the initial mass of the cluster using equation (3): $M_{in} = M(0)$. Although most of our comments are tailored to clusters with flat IMFs, some of the effects described here also apply to clusters with more conventional IMFs.

a) Stellar Winds

The winds from massive stars in a protocluster may create expanding shells of dense gas. There is considerable evidence for such structures near NGC 2070 ($\tau \approx 2 \times 10^6 \text{ yr}$) in the 30 Dor nebula (Cox and Deharveng 1983; Meaburn 1984). The total energy supplied by the wind of a single star is $E_w \approx \frac{1}{2} \dot{m}_w \tau_m v_w^2$, where \dot{m}_w is the mean mass-loss rate, τ_m is the main-sequence lifetime, and v_w is the velocity of the stellar wind. Using the empirical results of Abbott (1982), and power-law approximations to the mass-luminosity-radius relations for stars with $10 \lesssim m/M_\odot \lesssim 100$, we find $\dot{m}_w \approx 1.4 \times 10^{-7} (m/30 M_\odot)^{5.0} M_\odot \text{ yr}^{-1}$, $v_w \approx 3.0 \times 10^3 (m/30 M_\odot)^{0.14} \text{ km s}^{-1}$, and $\tau_m \approx 5.6 \times 10^6 (m/30 M_\odot)^{-0.9} \text{ yr}$. Combining these expressions gives $E_w \approx 7 \times 10^{49} (m/30 M_\odot)^{4.2} \text{ ergs}$. Castor, McCray, and Weaver (1975) have studied the structure and evolution of wind-driven bubbles in which the pressure of hot gas within the bubble is important. In this case, the kinetic energy of the expanding shell is $0.2E_w$. For comparison, the binding energies of the clusters in our sample are of the order of 10^{48} – 10^{49} ergs . In principle, therefore, the shell surrounding a single massive star would have enough energy to disrupt a protocluster. However, if cooling within the bubble is important, a much smaller fraction of the energy in the wind is available for driving the shell.

The most conservative condition for stellar winds to remove the gas from a protocluster is based on the assumption that the expanding shells are momentum rather than energy driven. The former case is also probably more realistic for bubbles in

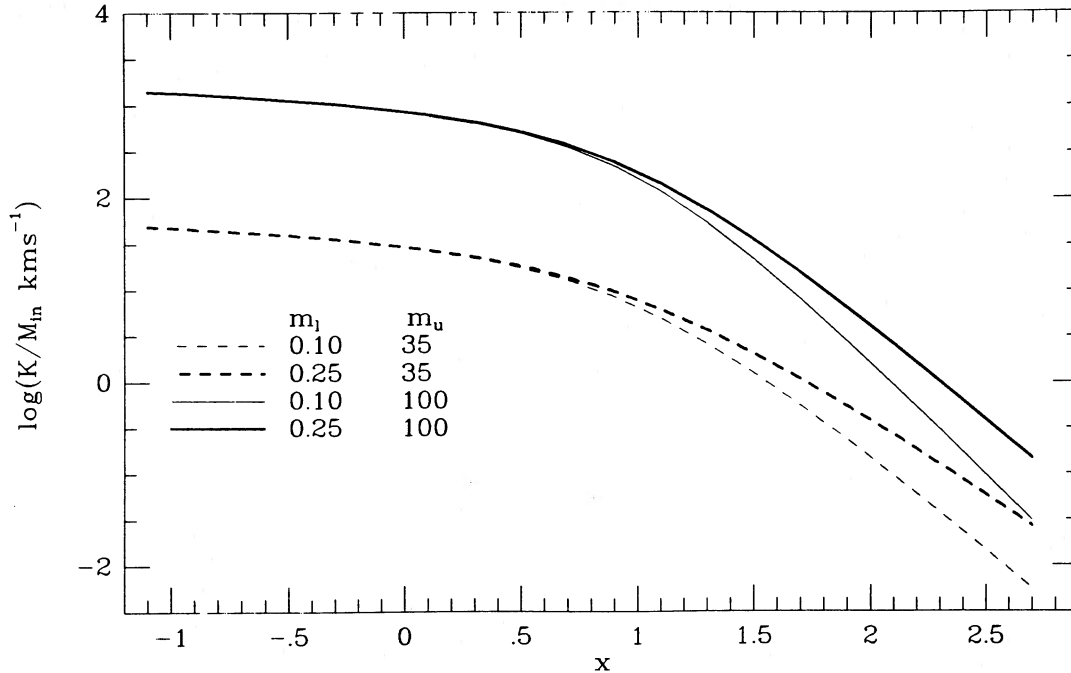


FIG. 9.—Ratio of the total momentum in stellar winds to the initial mass of a cluster as a function of the IMF slope. The different curves correspond to the upper and lower cutoffs indicated.

dense molecular clouds (Shull 1980; Elmegreen and Clemens 1985). Each massive star in a protocluster will initially produce an isolated bubble, but these bubbles will eventually merge to form larger ones. Once this occurs, the momenta in all the winds should be added. We therefore compute the quantity

$$K = A \int_{m_l}^{m_u} dmm^{-(1+x)} \dot{m}_w v_w \tau_m, \quad (5)$$

where \dot{m}_w , v_w , and τ_m vary with stellar mass m as above. Figure 9 shows $\log(K/M_{\text{in}} \text{ km s}^{-1})$ as a function of the IMF slope. A comparison with the entries in Table 3 indicates that K/M_{in} exceeds the velocity dispersions in the clusters for $x \lesssim 1.5$ and $m_u = 35 M_{\odot}$, or for $x \lesssim 2.0$ and $m_u = 100 M_{\odot}$. In these cases, there is enough momentum in the winds to remove or seriously rearrange the gas in a protocluster. The time scale for the gas to be expelled is probably of the same order as the period over which the stars formed. For steep IMFs, with $x \gtrsim 2$, stellar winds would have relatively little influence on a protocluster unless the gas within the expanding bubbles somehow remained hot (see the above discussion of energy-driven shells).

b) Supernovae

We first estimate the number of supernovae that would have occurred in a cluster with a mass function given by equation (2). This is

$$N_{\text{sn}} = A \int_{m_s}^{m_u} dmm^{-(1+x)}, \quad (6)$$

where m_s , the minimum mass required for a star to explode, is taken to be $12 M_{\odot}$. Figure 10 shows $\log(N_{\text{sn}} M_{\odot}/M_{\text{in}})$ as a function of x with the adopted values of m_l and m_u . For flat IMFs, with $x \lesssim 1$, we find $N_{\text{sn}} \approx (1-4) \times 10^{-2} (M_{\text{in}}/M_{\odot})$. As shown below, the initial masses of the clusters in our sample must have been a few times larger than their present masses,

and this estimate together with the masses listed in Table 3 implies $N_{\text{sn}} \approx 10^2-10^4$. For steep IMFs, with $x \gtrsim 2$, the numbers of supernovae are smaller by factors of at least 30.

The effect on a protocluster of a large number of supernovae depends critically on whether the explosions occur before or after most of the gas was removed (e.g., by stellar winds). In Paper I we argued that the *minimum* time scale on which star formation could be synchronized is the crossing time; for the clusters in our sample this is $1-20 \times 10^6$ yr (Table 3). The narrow spread in the luminosities of supergiants in the clusters implies that the *maximum* interval over which stars formed is $\sim 10 \times 10^6$ yr (Robertson 1974a). For comparison, the main-sequence lifetimes of the progenitors of the supernovae range from 2 to 12×10^6 yr. These time scales are such that most of the supernovae could have occurred while the protoclusters were still mainly gaseous. (The predicted number of supernovae in clusters with flat IMFs is so great that even if the high-mass stars formed systematically later than the low-mass stars, a significant number would still have formed early.) The following arguments explore the effects of supernovae in a gaseous protocluster, but encounter serious difficulties, suggesting that the majority of the supernovae occurred after most of the gas in the protocluster had been consumed by star formation or expelled by stellar winds.

The total mass of heavy elements produced and ejected by the supernovae is

$$\Delta M_Z = A \int_{m_s}^{m_u} dmm^{-x} p(m), \quad (7)$$

where $p(m)$ is the yield of a star with an initial mass m . We use a simple approximation to the detailed calculations of explosive nucleosynthesis by Weaver and Woosley (1980):

$$p(m) = \begin{cases} 0.5(1 - m_s/m) & \text{for } m \geq m_s; \\ 0 & \text{for } m < m_s. \end{cases} \quad (8)$$

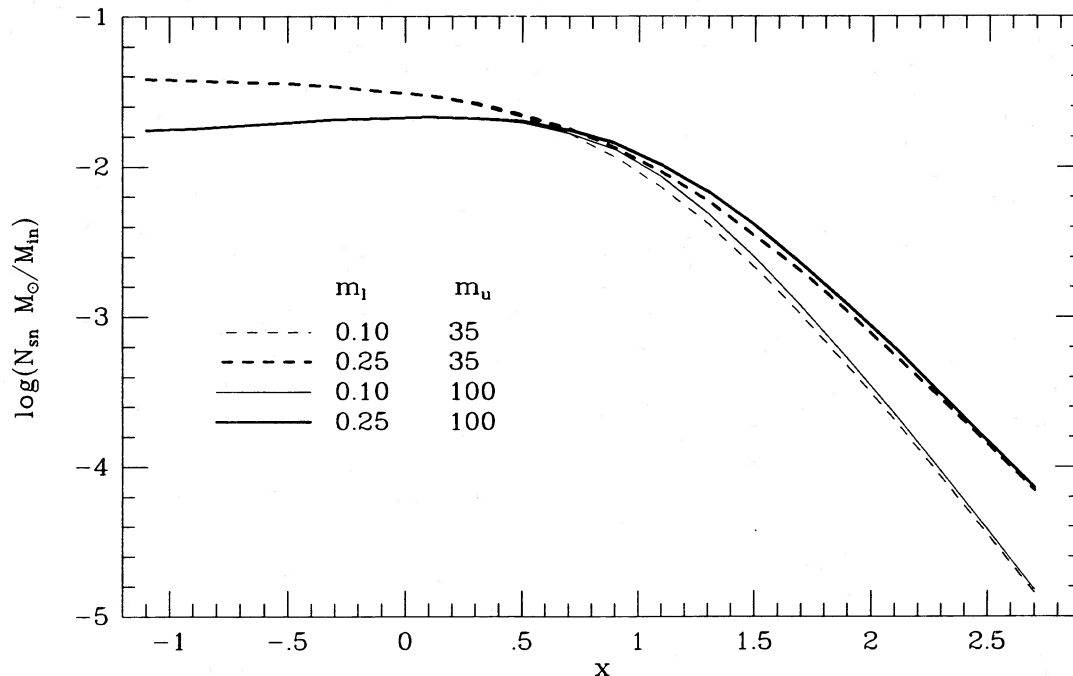


FIG. 10.—Ratio of the number of supernovae to the initial mass of a cluster, as a function of the IMF slope. The different curves correspond to the upper and lower cutoffs indicated.

The resulting dependence of $\log(\Delta M_Z/M_{in})$ on x is plotted in Figure 11. For flat IMFs, we find $\Delta M_Z \approx (6-35) \times 10^{-2} M_{in}$. This is valid whether the supernovae occur when the proto-clusters are mainly gaseous or mainly stellar. In the former case, some of the heavy elements might be retained whereas in the latter case they would enrich the surrounding interstellar medium but not the clusters. If the heavy elements were retained and mixed with the gas in a protocluster, the change in the mean metallicity would be $\Delta Z \approx \Delta M_Z/M_{gas}$ or,

from the results above, $\Delta Z \approx (3-17)(M_{in}/M_{gas})Z_{\odot}$. For reasonable values of the efficiency of star formation, $\frac{1}{3} \lesssim M_{in}/M_{gas} \lesssim 1$, this implies $\Delta Z \gtrsim Z_{\odot}$. Since the observed metallicities of the clusters are below solar, most of the supernovae must have occurred after the gas in the protoclusters was either used up or expelled. For steep IMFs, with $x \gtrsim 2$, the predicted enrichment is negligible, and no conclusions can be drawn about the sequence of supernovae explosions and gas removal.

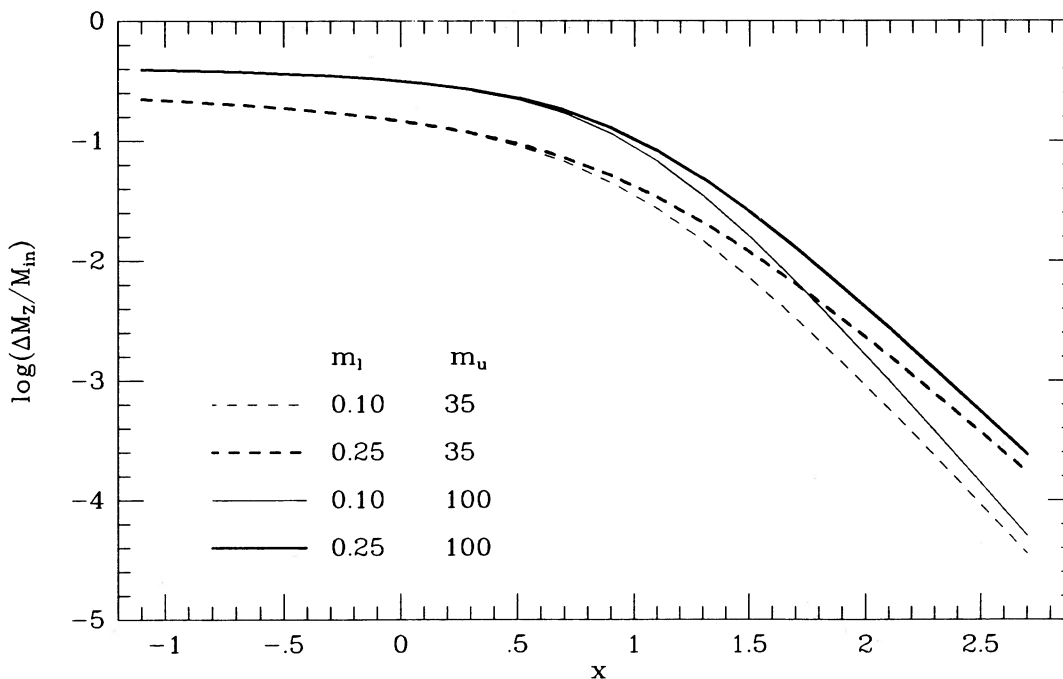


FIG. 11.—Ratio of the mass of metals produced by supernovae, to the initial mass of a cluster, as a function of the IMF slope. The different curves correspond to the upper and lower cutoffs indicated.

Supernovae would have been very effective in expelling from a protocluster any gas that had not already been removed by stellar winds. To show this we first estimate the mass swept up by an isolated supernova remnant. In the isothermal or snow-plow phase, in which the remnant spends most time, the result is

$$M_s = (0.59/v_s)(kT_i/\mu)^{-1/2} E_0. \quad (9)$$

Here E_0 is the initial energy of the ejected envelope, $T_i \approx 1 \times 10^6$ K is the temperature at which the remnant makes the transition from the adiabatic to isothermal phase, $\mu \approx 0.6m_H$ is the mean mass per particle of ionized gas, and v_s is the instantaneous velocity of the remnant. (Eq. [9] can be derived from the formulae in § 12.2 of Spitzer 1978). The only dependence of M_s on the density of the ambient medium is through T_i , which is weak enough to be ignored here. The expansion of the remnant continues until v_s is approximately equal to the effective velocity dispersion in the surrounding gas (probably turbulent). This is not known precisely but is likely to be close to the stellar velocity dispersion in the clusters today, 1–5 km s⁻¹, which implies $M_{\max} \approx (6-30) \times 10^4 (E_0/10^{51} \text{ ergs}) M_\odot$.

We now consider the effect of many supernovae on the gas in a protocluster. To the extent that E_0 is independent of the masses of the progenitor stars, the total mass swept up, either before or after the remnants overlap, is simply $N_{\text{sn}} M_s$. Using the maximum mass of the remnants derived above, and the relation shown in Figure 10, we find that $N_{\text{sn}} M_{\max}$ exceeds the initial mass of a protocluster, M_{in} , for $x \lesssim 2.7$. This suggests that, with either the flat IMFs we have found or the steep IMFs found by Mateo, there would have been enough supernovae to remove or rearrange most of the gas in the protoclusters. The heavy elements produced by the supernovae would also be expelled, and later supernovae would essentially explode into a vacuum. We conclude that very little self-enrichment of the protoclusters is possible even when the IMFs are flat. Another consequence of these arguments is that

the time scale for star formation cannot be much longer than a few $\times 10^6$ yr, the main-sequence lifetimes of the progenitors of the supernovae. This is comparable to the lower limits on age spreads estimated by Robertson (1974a).

c) Stellar Ejecta

Clusters with flat IMFs would have lost a significant fraction of their masses in the form of ejecta from massive stars over and above the loss of gas before it was incorporated into stars (Applegate 1986; Chernoff and Weinberg 1988). Using equation (3), we have calculated the total mass in stars $M(\tau)$ as a function of the age τ and IMF slope x . Figure 12 shows $\log [M(\tau)/M_{\text{in}}]$ for $\tau = 3 \times 10^7$ yr, which is close to the age of NGC 1866, and equal to the ages of the other clusters in our sample. For $x \lesssim 0$, more than two thirds of the mass is lost, whereas for $x \gtrsim 1$, less than one third of the mass is lost. As discussed in Paper I, a cluster or a protocluster that was initially limited by the tidal field of the LMC would, after mass loss by any mechanism, spill over its Roche limit. With flat IMFs, the unbound halos of the LMC clusters could be produced solely by expansion due to mass loss from stellar evolution.

VII. CONCLUSIONS

We have determined the IMFs of six young rich clusters in the LMC from star counts on photographic plates with different limiting magnitudes. Over the range of stellar masses $1.5 \lesssim m/M_\odot \lesssim 6$, we find very flat IMF slopes: $-0.2 \lesssim x \lesssim 0.8$. There may be small variations from one cluster to another, but they are within the observational uncertainties. Our results contrast with those of Mateo (1988), who finds steep IMFs ($x \approx 2.5$) for a different sample of clusters in the Magellanic Clouds. We have considered possible explanations for the discrepancy between his results and ours, including differences in the luminosity functions, and the methods used to convert

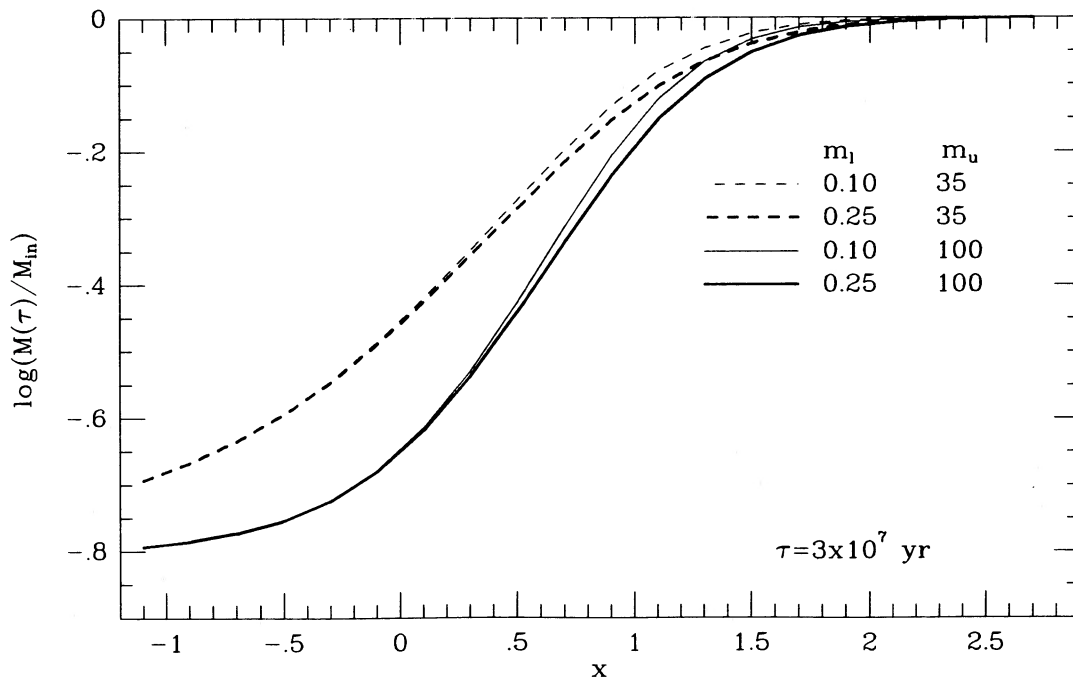


FIG. 12.—Ratio of present to initial mass of a cluster as a function of the IMF slope. The assumed age is 3×10^7 yr. The different curves correspond to the upper and lower cutoffs indicated.

them to mass functions. There are no obvious inconsistencies, although the comparison between the two studies is very limited. If both sets of results are correct, there must be large variations in the IMFs.

The large fields afforded by photographic plates ensure that our estimates of the background densities and luminosity functions are statistically well determined and allow us to work in regions of the clusters where crowding is not a serious problem. CCDs have the advantage that the magnitudes of individual stars can be determined with great accuracy. They are, however, restricted to small fields, and in order to sample enough stars for statistically valid results, the luminosity functions must be determined in crowded regions of the clusters where incompleteness is severe. The most reliable determinations of luminosity functions may ultimately come from "mosaics" of CCD frames covering large areas of the clusters and backgrounds, thereby combining the advantages of photographic plates and single CCD frames.

The flat IMFs we have found for the young LMC clusters imply smaller mass-to-light ratios than previously assumed and reinforce our conclusions from Paper I that the clusters have unbound halos. Our results are consistent with the correlation between the metallicity and IMF slope noted by McClure *et al.* (1986) for Galactic globular clusters. Flat IMFs also have the following implications concerning the formation and early evolution of the clusters: (1) Stellar winds would have been very important in restructuring and expelling the gas from a protocluster. (2) There would have been many

supernovae early in the history of a cluster. Constraints on the amount of self-enrichment compatible with the observed metallicities of the clusters suggest that the majority of supernovae occurred after most of the gas had either been converted into stars or expelled. This in turn suggests that the time scale for star formation in the protoclusters was not much greater than a few $\times 10^6$ yr. (3) Even after all the unused gas in a protocluster was expelled, there would have been a significant amount of mass lost through stellar evolution. Mass loss of any sort would cause the clusters to expand past their Roche limits, and could account for the unbound halos found in Paper I. Once again we emphasize that these conclusions are based on simple extrapolations of the observed IMFs to masses well above the present turnoffs.

We are grateful to Johannes Andersen for communicating unpublished photometry of NGC 1866, to Janet Yamanaka for supplying the mass-to-light ratios plotted in Figures 8a and 8b, and to Joanne Fisher for assistance with the star counts. We thank Robert Lupton, Mario Mateo, Nolan Walborn, and Rick White for valuable comments and discussions, and John Scalo for a very helpful referee's report. S. M. F. and K. C. F. are grateful to the Institute for Advanced Study for hospitality during various phases of this work. R. A. W. E. is supported by grants from the Corning Glass Works Foundation to the Institute for Advanced Study, and by NASA/Goddard Contract NAS-29225.

REFERENCES

- Abbott, D. C. 1982, *Ap. J.*, **259**, 282.
 Andersen, J., Blecha, A., and Walker, M. F. 1984, *M.N.R.A.S.*, **211**, 695.
 Applegate, J. H. 1986, *Ap. J.*, **301**, 132.
 Becker, S. A. 1981, *Ap. J. Suppl.*, **45**, 475.
 Becker, S. A., and Mathews, G. J. 1983, *Ap. J.*, **270**, 155.
 Becker, S. A., Mathews, G. J., and Brunish, W. M. 1984, in *IAU Symposium 105, Observational Tests of the Stellar Evolution Theory*, ed. A. Maeder and A. Renzini (Dordrecht: Reidel), p. 83.
 Bertelli, G., Bressan, A., Chiosi, C., and Angerer, K. 1986, *Astr. Ap. Suppl.*, **66**, 191.
 Brück, M. T. 1984, in *IAU Symposium 108, Structure and Evolution of the Magellanic Clouds*, ed. S. van den Bergh and K. de Boer (Dordrecht: Reidel), p. 97.
 Burki, G. 1977, *Astr. Ap.*, **57**, 135.
 Butcher, H. R. 1977, *Ap. J.*, **216**, 372.
 Castor, J., McCray, R., and Weaver, R. 1975, *Ap. J. (Letters)*, **200**, L107.
 Chernoff, D., and Weinberg, M. 1988, in preparation.
 Chiosi, C., and Pigatto, L. 1986, *Ap. J.*, **308**, 1.
 Cohen, J. G. 1982, *Ap. J.*, **258**, 143.
 Conti, P. S., Garmany, C. D., and Massey, P. 1986, *A.J.*, **92**, 48.
 Cox, P., and Deharveng, L. 1983, *Astr. Ap.*, **117**, 265.
 Da Costa, G. 1982, *A.J.*, **87**, 990.
 D'Antona, F. 1987, *Ap. J.*, **320**, 653.
 Elmegreen, B. G., and Clemens, C. 1985, *Ap. J.*, **294**, 523.
 Elson, R. A. W., and Fall, S. M. 1985a, *Ap. J.*, **299**, 211.
 ———. 1985b, *Pub. A.S.P.*, **97**, 692.
 Elson, R. A. W., Fall, S. M., and Freeman, K. C. 1987, *Ap. J.*, **323**, 54 (Paper I).
 Flower, P. J., Geisler, D., Hodge, P., and Olszewski, E. W. 1980, *Ap. J.*, **235**, 769.
 Flower, P. J., and Hodge, P. W. 1975, *Ap. J.*, **196**, 369.
 Freedman, W. L. 1985, *Ap. J.*, **299**, 74.
 Freeman, K. C. 1977, in *The Evolution of Galaxies and Stellar Populations*, ed. B. M. Tinsley and B. Larson (New Haven: Yale University Observatory), p. 133.
 Freeman, K. C., Illingworth, G., and Oemler, A. 1983, *Ap. J.*, **272**, 488.
 Hardy, E., Buonanno, R., Corsi, C. E., Janes, K. A., and Schommer, R. A. 1984, *Ap. J.*, **278**, 592.
 Harris, W. E., and Hesser, J. E. 1985, in *IAU Symposium 113, Dynamics of Star Clusters*, ed. J. Goodman and P. Hut (Dordrecht: Reidel), p. 81.
 Hodge, P. W. 1984, *Pub. A.S.P.*, **96**, 947.
 Humphreys, R. M., and McElroy, D. B. 1984, *Ap. J.*, **284**, 565.
 Iben, I., and Renzini, A. 1983, *Ann. Rev. Astr. Ap.*, **21**, 271.
 King, I., Hedemann, E., Hodge, S. M., and White, R. E. 1968, *A.J.*, **73**, 456.
 Lucke, P. B. 1974, *Ap. J. Suppl.*, **28**, 73.
 Lupton, R. H., Elson, R. A. W., Fall, S. M., and Freeman, K. C. 1988, in preparation.
 Mateo, M. 1988, *Ap. J.*, **331**, 261.
 McClure, R. D., *et al.* 1986, *Ap. J. (Letters)*, **307**, L49.
 ———. 1987, private communication.
 Meaburn, J. 1984, *M.N.R.A.S.*, **211**, 521.
 Melnick, J. 1985, in *Star Forming Dwarf Galaxies and Related Objects*, ed. D. Kunth, T. X. Thuan, and J. T. Van Thanh (Paris: Editions Frontieres), p. 171.
 Nelson, M., and Hodge, P. 1983, *Pub. A.S.P.*, **95**, 5.
 Penny, A. J., and Dickens, R. J. 1986, *M.N.R.A.S.*, **220**, 845.
 Persson, S. E., Aaronson, M., Cohen, J. G., Frogel, J. A., and Mathews, K. 1983, *Ap. J.*, **266**, 105.
 Robertson, J. W. 1974a, *Ap. J.*, **191**, 67.
 ———. 1974b, *Astr. Ap. Suppl.*, **15**, 261.
 Sandage, A., and Tammann, G. 1974, *Ap. J.*, **190**, 525.
 Scalo, J. 1986, *Fund. Cosmic Phys.*, **11**, 1.
 Schommer, R. A., and Geisler, D. 1988, in *IAU Symposium 126, Globular Cluster Systems in Galaxies*, ed. J. Grindlay and A. G. Davis Philip (Dordrecht: Reidel), p. 577.
 Schommer, R. A., Olszewski, E. W., and Aaronson, M. 1984, *Ap. J. (Letters)*, **285**, L53.
 Shull, J. M. 1980, *Ap. J.*, **238**, 860.
 Spitzer, L. 1978, *Physical Processes in the Interstellar Medium* (New York: Wiley).
 Stryker, L. L., and Butcher, H. R. 1981, in *IAU Colloquium 68, Astrophysical Parameters for Globular Clusters*, ed. A. G. Davis Philip and D. S. Hayes (Schenectady: Davis), p. 255.
 Vandenberg, D. A. 1985, *Ap. J. Suppl.*, **58**, 711 (VdB).
 Vandenberg, D. A., and Bridges, T. J. 1984, *Ap. J.*, **278**, 679.
 Vogt, N. 1971, *Astr. Ap.*, **11**, 359.
 Walborn, N. R. 1984, in *IAU Symposium 108, Structure and Evolution of the Magellanic Clouds*, ed. S. van den Bergh and K. de Boer (Dordrecht: Reidel), p. 243.
 Walker, M. F. 1974, *M.N.R.A.S.*, **169**, 199.
 Weaver, I. A., and Woosley, S. E. 1980, *Ann. NY Acad. Sci.*, **336**, 335.
 Yamanaka, J. 1987, private communication.

REBECCA A. W. ELSON: Institute for Advanced Study, Princeton, NJ 08540

S. MICHAEL FALL: Space Telescope Science Institute, 3700 San Martin Drive, Baltimore, MD 21218

KENNETH C. FREEMAN: Mount Stromlo Observatory, Private Bag, Woden P.O., A.C.T. 2606, Australia